Metal-organic-coordinated supramolecular material filled hollow core photonic crystal fiber for temperature sensor

Jiarong Zheng (郑家容)[1], Yongqin Yu (于永芹)[2*], Chenlin Du (杜晨林)[1], Peiguang Yan (闫培光)[1], Mei Pan (潘 梅)[3], Jishun Wang (王继顺)[1], and Zhuoye Liu (刘卓业)[2]

[1]*Shenzhen Key Laboratory of Laser Engineering, College of Electronic Science and Technology, Shenzhen University, Shenzhen 518060, China*

[2]*College of Physical Science and Technology, Shenzhen University, Shenzhen 518060, China*

[3]*MOE Laboratory of Bioinorganic and Synthetic Chemistry, State Key Laboratory of Optoelectronic Materials and Technologies, School of Chemistry and Chemical Engineering, Sun Yat-Sen University, Guangzhou 510275, China*

**Corresponding author: yuyq@szu.edu.cn*

Received April 5, 2012; accepted August 13, 2012; posted online December 20, 2012

A novel hollow core photonic crystal fiber (HCPCF) temperature sensor that is based on intensity modulation and metal-organic-coordinated Co-cage supramolecular material filled in the air holes of the fiber is introduced. Temperature-dependent character of the structure in the range of 90 to 190 °C has been investigated. The numerical analyses show that the confinement loss is both decreased linearly with temperature at 1 064 and 1 550 nm. For a 6.5-cm long HCPCF, the sensitivity of temperature is experimentally determined to be 9.5×10^{-2} dB/°C at 1 064 nm, and 7.9×10^{-2} dB/°C at 1 550 nm, respectively.

OCIS codes: 060.5295, 160.6840, 060.2370.

doi: 10.3788/COL201210.S20611.

Photonic crystal fibers (PCFs), a novel class of fibers offer new and exciting possibilities in many application fields. Recently, hollow core photonic crystal fiber (HCPCF) has attracted lots of attention for its particular structure, which consists of a central air hole and several layers of aligned cladding holes. The aligned cladding holes form periodic variation of the refraction index, generating a photonic band gap (PBG) for the limitation of photon. With properly designed core defect, light can propagate with a value of propagation constant β that falls within the band gap of the PCF[1]. While filling with materials, the air holes provided natural places for interaction between propagating light and materials. Recently, there is growing interest in exploring PCFs as sensor devices, including gas[2,3], liquid[3−10], and solid filled structures[11−13]. According to different properties of filled materials, the sensors based on HCPCFs have realized different applications. Ritari *et al*. realized a gas PCF sensor by detecting the absorption character of acetylene and methane[2]. Yan *et al*. showed a PCF infiltrating nano particles, which provided a platform for surface-enhanced Raman scattering (SERS) sensors[4]. Smolka *et al*. investigated the fluorescence phenomenon of nanoliter dye sample volumes in PCF[11]. Qian *et al*. proposed an ethanol-filled PCF device for the detection of temperature and the temperature sensitivity reaches up to − 0.35 nm/°C[9]. The outstanding advantages of these PCF-based sensors are simple design, high stability, and high sensitivity.

In this letter, the optical response of a HCPCF filled with a kind of material called metal-organic-coordinated Co-cage supramolecular (representing as Co-cage-filled HCPCF) is studied. The refractive index of Co-cage is sensitive to temperature, and linearly changes as temperature alters from 90 to 190 °C. The transmission power of Co-cage-filled HCPCF is used as temperature sensor signal at 1 064 and 1 550 nm. It is different from the material-filled PCF sensors reported in references with the wavelength as sensitivity signal. The numerical calculations and experiments are discussed in the letter.

The full-vector finite element method (FEM) is used to calculate the mode field distributions of PCFs. Perfectly matched layer (PML) is served as the boundary condition. The confinement loss and the eigenvalue equation of propagation are solved in the Perpendicular Hybrid-Mode. The structure parameters of PCF are shown as following: the pitch Λ = 3.3 μm, cladding air hole diameter d_1=2.2 μm, central core diameter d_2=7.6 μm, and the cladding diameter d_3=130 μm. Co-cage, a temperature sensitive material, is filled in air holes of PCF. The refractive index of Co-cage at room temperature (26 °C) is measured by Abbé refractometer to be 1.3524. Its thermo-optic coefficient α is obtained to be $-5.74\times10^{-5}\text{K}^{-1}$. Transmission loss of this structure is caused by intrinsic material absorption, confinement loss as well as loss arising by fabrication. The confinement loss is relative with the structure of PCF, the mode effective refractive index of PCF, and the propagating light. It can be expressed by[7]

$$P_{\mathrm{L}} = 20\,\mathrm{lg(e)}k_0\mathrm{Im}\left[n_{\mathrm{eff}}\right]L, \tag{1}$$

where P_{L} refers to confinement loss, L is the length of fiber, k_0 is the wave vector of propagating light, and n_{eff} is the mode effective refractive index of PCF. Figure 1 shows the fundamental mode field distributions of the Co-cage-filled HCPCF with input wavelengths of 1 064 and 1 550 nm at 90 °C, respectively. It can be seen from Fig. 1 that more optical power is distributed in the cladding of PCF in the case of input wavelength at 1 064 nm than that at 1 550 nm.

The mode effective refractive indexes, as a function of temperature from 90 to 190 °C at 1 064 and 1 550 nm, are shown in Fig. 2. The real part of the mode effective refractive indexes, referring to propagation constant, is inversely proportional to temperature. The confinement loss, which is relative with the imaginary part of n_{eff}, is directly proportional to temperature. The temperature sensitivities of confinement loss are estimated by using linearly regression fits, which are −50.11 dBm/m/°C at 1 064 nm and −24.34 dBm/m/°C at 1 550 nm, respectively.

The transmission property of Co-cage is measured in the quartz cuvette by spectrophotometer. The spectrum from 300 to 1 600 nm is described in Fig. 3. It can be seen that the absorption at near infrared (NIR) is weaker than that at visible wavelengths. The transmission at 1 064 nm is 51% and 73% at 1 550 nm from Fig. 3.

So in our experiments, to gain the stronger signal intensity, we took into account the transmission of Co-cage and applied two NIR lasers working at 1 064 and 1 550 nm as input sources, which are cheap and widely used.

The optical microscopic image of the end of HCPCF used in the experiments is shown in Fig. 4. The solution is achieved by full dissolving 0.0159-g Co-cage in 3-ml ethanol. The prepared HCPCF is then inserted into the solution. By capillary force and air pressure, all the air holes of the HCPCF are filled with solution. Ethanol is also the thermo-optic material whose boiling point is 78 °C. In order to eliminate the effect of ethanol, we start the measurement at 90 °C. Only Co-cage remains in the air holes of HCPCF. To enhance the interaction between Co-cage and propagating light, perfusions are carried out repeatedly by thrice to guarantee the full infiltration.

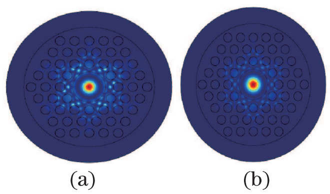

Fig. 1. Mode field distribution of Co-cage-PCF at 90 °C: (a) at 1 064 nm; (b) at 1 550 nm.

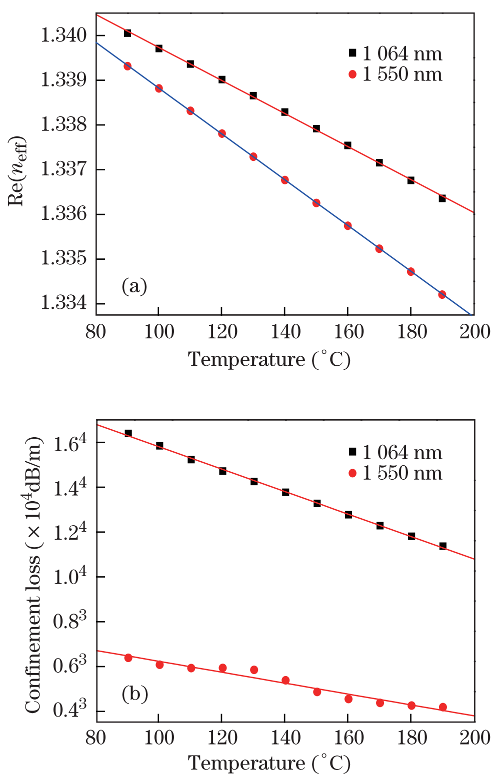

Fig. 2. (a) Dependent of the real part of mode effective refractive index of Co-cage-filled HCPCF on temperature and (b) the dependent of the confinement loss on temperature, which is related with the imaginary part of the effective refractive index.

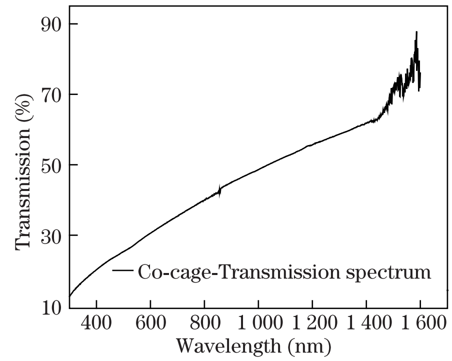

Fig. 3. Transmission spectrum of Co-cage from 300 to 1 600 nm.

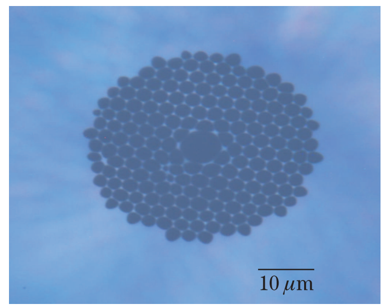

Fig. 4. Optical microscopic image of the end of HCPCF.

In our experiments, the refractive index of Co-cage is lower than that of silica. The Co-cage-filled HCPCF is made up of lower index solid core surrounded by higher index cladding. Light is still guided through this fiber by bandgap effect. Because the refractive index of Co-cage is changed by varying temperature, the mode effective refractive index and confinement loss of Co-cage-filled HCPCF are also temperature dependent.

To measure the temperature dependence, a Co-cage-filled HCPCF with a length of 6.5 cm is used. One end of PCF is spliced with single mode fiber (SMF), and the other is spliced with multimode fiber (MMF). The PCF is then placed in the V-groove of a cylindrical heater (from room temperature to 190 °C, ± 0.5 °C) to avoid bending effects. Laser at different wavelengths (1 064 and 1 550 nm) are used as input sources. The input source passes through a 10-dB SMF coupler into one end of the HCPCF. The opposite end of PCF is coupled to an optical power meter (AI9402A, with measured range from −90∼3 dBm). The power stability of input source is detected through the other end of the 10-dB coupler. Transmission power is recorded from 90 to 190 °C at 10 °C intervals. The output spectrum and power

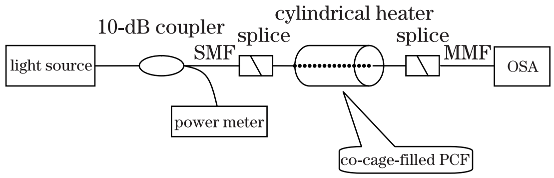

Fig. 5. Scheme of experimental setup for temperature sensor.

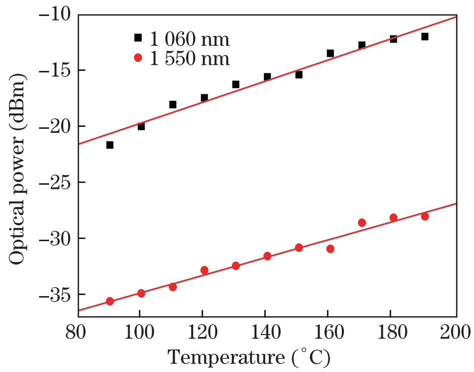

Fig. 6. Temperature dependence of transmission power for Co-cage-filled HCPCF at 1 064 and 1 550 nm.

are detected by an optical spectrum analyzer (OSA) (ADVANTEST Q8384). Figure 5 shows the scheme of the experimental setup for the temperature-dependence measurements of Co-cage-filled HCPCF.

The experimental results of the transmission power at 1 064 and 1 550 nm as a function of temperature from 90 to 190 °C are described in Fig. 6, where temperature dependence is obvious. The temperature sensitivities are estimated by using linearly regression fits, which are 9.5×10^{-2} dB/°C at 1 064 nm and 7.9×10^{-2} dB/°C at 1 550 nm. The linearity of the temperature sensitivities is high and the linear correlations are $R = 0.98296$ at 1 064 nm and $R = 0.98802$ at 1 550 nm within temperature range from 90 to 190 °C. The output power is directly proportional to the temperature, which infers that the confinement loss decreases with temperature. It coincides well with the numerical analysis. As the result shows, the temperature sensitivity of transmission power is relative higher at 1 064 nm than that at 1 550 nm. This can be seen from Fig. 1 that more optical power is spread into the cladding region at 1 064 nm than that at 1 550 nm. Thus the interaction between light and Co-cage at 1 064 nm is much more sufficient than that at 1 550 nm, resulting higher temperature sensitivity.

Interaction between light and Co-cage filled in HCPCF in the range of 90 to 190 °C has been investigated. Transmission spectra of Co-cage at 1 064 and 1 550 nm are 51 % and 73 %, respectively. Lasers at 1 064 and 1 550 nm are used as input sources in our experiments. The numerical analyses show the real part of mode effective refractive index and the confinement loss of Co-cage-filled HCPCF are linearly dependent on temperature at 1 064 and 1 550 nm, respectively. Experiments are conducted to be coincident with theory that the output power is linearly increasing with temperature. The slopes of temperature dependent intensity-curve are 9.5×10^{-2} dB/°C at 1 064 nm, and 7.9 $\times10^{-2}$ dB/°C at 1 550 nm for a 6.5-cm-long HCPCF, respectively. The temperature sensitivity of transmission power is relative higher at 1 064 nm than that at 1 550 nm. This structure shows its prospect as temperature sensor.

This work was supported by Shenzhen Science and Technology Project (No. JC201005280473A) and the open project of Shenzhen key lab of sensor technology (No. SST201201).

References

1. J. C. Knight, J. Broeng, T. A. Birks, and P. St. J. Russell, Science **282,** 1476 (1998).
2. T. Ritari, J. Tuominen, H. Ludvigsen, J. C. Petersen, T. Sørensen, T. P. Hansen, and H. R. Simonsen, Opt. Express **12,** 4080 (2004).
3. J. M. Fini, Meas. Sci. Technol. **15,** 1120 (2004).
4. H. Yan, J. Liu, C. Yang, G. Jin, C. Gu, and L. Hou, Opt. Express **16,** 8300 (2008).
5. H. Yan, C. Gu, C. Yang, J. Liu, G. Jin, J. Zhang, L. Hou, and Y. Yao, Appl. Phys. Lett. **89,** 204101 (2006).
6. Y. Zhang, C. Shi, C.Gua, L. Seballos and J. Z. Zhang, Appl. Phys. Lett. **90,** 193504 (2007).
7. Y. Yu, X. Li, X. Hong, Y. Deng, K. Song,Y. Geng, H. Wei, and W. Tong, Opt. Express **18,** 15383 (2010).
8. W. Ye, L. L. Irene, C. R. Shuang, and P. Z. Jian, in *Proceedings of the International Conference on Microwave and Millimeter Wave Technology* (*ICMMT, 2008*) **2,** 890 (2008).
9. W. Qian, C. L. Zhao, C. C. Chan, L. Hu, T. Li, W. C. Wong, P. Zu, and X. Dong, Sensors J. **12,** 2593 (2012).
10. W. Qian, C. Zhao, S. He, X. Dong, S. Zhang, Z. Zhang, S. Jin, J. Guo, and H. Wei, Opt. Lett. **36,** 1548 (2011).
11. S. Smolka, M. Barth, and O. Benson, Opt. Express **15,** 12783 (2007).
12. B. Larrión, M. Hernáez, F. J. Arregui, J. Goicoechea, J. Bravo, and I. R. Matías, Journal of Sensors **2009,** 932471 (2009).
13. C. Markos, K. Vlachos, and G. Kakarantzas, Opt. Mater. Express **2,** 929 (2012).